Hemilabile Thioether Ligands Based on Pyrimidine and/or Pyridine Derivatives that Interconvert between *N*,*S*- and *N*-Coordination in Congested Ruthenium(II) Complexes

Giuseppe Tresoldi,*[a] Laura Baradello,[a] Santo Lanza,[a] and Paola Cardiano[a]

Keywords: Ruthenium / Pyridine thioether / Pyrimidine thioether / *N*,*S*-Coordination / *N*-Coordination

The thioether ligands **L** [**L** = 2-pyridylmethyl 2′-pyridyl sulfide ($\mathbf{L_1}$), 2-pyridylmethyl 2′-pyrimidyl sulfide ($\mathbf{L_2}$) and 2-pyridylmethyl 2′-(4-methylpyrimidyl) sulfide ($\mathbf{L_3}$)] react with *cis*-[Ru(*N*,*N*-diimine)$_2$Cl$_2$] {diimine = 2,2′-bipyridine (bipy), di-2-pyrimidyl sulfide (dprs), 2,2′-bis(5-ethylpyrimidyl) sulfide (5edprs)} to give compounds [Ru(*N*,*N*-diimine)$_2$L][PF$_6$]$_2$ {diimine = bipy, **L** =$\mathbf{L_1}$ (**1**), $\mathbf{L_2}$ (**2**), $\mathbf{L_3}$ (**3**); diimine = dprs, **L** = $\mathbf{L_1}$ (**4**); diimine = 5edprs, **L** = $\mathbf{L_1}$ (**5**); diimine = dprs, **L** = $\mathbf{L_2}$ (**6**), **L** = $\mathbf{L_3}$ (**7**); diimine = 5edprs, **L** = $\mathbf{L_2}$ (**8**), **L** = $\mathbf{L_3}$ (**9**)}. NMR investigations show that these potentially tridentate ligands act as *N*,*S*-bidentate species, to form a five-membered RuSCCN(*Ru–N*) ring, and in certain cases, as *N*-monodentate species coordinated to the ruthenium through the 2-pyridylmethyl group. The *N*,*S*-chelated species contain chiral sulfur and ruthenium atoms with (*R*) and (*S*), and Δ and Λ configurations, respectively. Two invertomers and two sets of NMR signals in the slow-exchange region are expected. However, the low-temperature ^{1}H NMR spectra show that sulfur inversion is fast. The variable-temperature ^{1}H NMR spectra allow two species to be observed (**6a** + **6b**, **7a** + **7b**, **8a** + **8b** and **9a** + **9b**), which exhibit different abundances. In the minor species (**6b**, **7b**, **8b**, and **9b**), $\mathbf{L_2}$ or $\mathbf{L_3}$ exhibits an *N*-monodentate coordination, while in the major species, the usual *N,S*-coordination. At low temperatures, the population ratio is about 85:15, while when the temperature increases, the abundance of the minor species grows rapidly. The one-dimensional band-shape analysis of the exchanging methylene proton signals shows that the energy-barrier for the interchange process ($\Delta G^{\#}_{298}$) for **6a** + **6b**, **7a** + **7b**, **8a** + **8b**, and **9a** + **9b** is practically the same (ca. 59.5 kJ·mol^{-1}), while the $\Delta S^{\#}$ values are negative or near to zero. The possible mechanisms for the process are discussed. The NMR spectroscopic findings strongly support the formation of an *N*,*N*-chelated labile intermediate.

Introduction

The coordination chemistry of chelated ligands containing mixed functionalities in transition-metal complexes is an active area of research. In particular, the chemistry of hemilabile ligands, which contain both inert and labile groups, has received considerable attention.[1] Since one group bonds strongly to a metal center, the substitutionally labile group, which can be displaced from the metal center, remain available for recoordination. Thus the hemilability of a chelate can be observed as a dynamic process that involves the dissociation and recoordination of weakly bound moieties. When the hemilabile ligand contains two or more weakly bonding groups, it may undergo intramolecular ligand-exchange reactions. These processes often have been referred to as “wind-screen wiper” or “tick-tock” mechanisms,[2–9] and “opening and closing” or “rotation” mechanisms.[8–10] Furthermore, hemilability through ligand-interchange reactions involving equilibria between weakly bonding groups of the ligand and coordinating counterions, small molecules, or solvent molecules has been observed.[10,11]

There are many reasons for studying hemilabile ligands. Since these ligands can furnish open coordination sites and stabilize reactive transition-metal centers throughout the course of the reaction, their complexes can be utilized in catalytic reactions. Complexes containing hemilabile ligands have been shown to be active, for example, toward hydrogenation,[12] methanol carbonylation,[13] hydroformylation,[14] dimerization of ethene,[15] isomerization of alkene,[16] allylation,[17] and epoxidation of alkenes.[18] Furthermore, the labile fragments of these ligands are often displaced easily and reversibly from the metal center by small molecules, and the corresponding complexes are useful for small molecule activation[19] and sensing.[20]

N-heterocyclic donors are often good ligands for many transition-metal centers, and ligands containing inert *N*-heterocyclic moieties, in particular, pyridine or bipyridine groups are the most common type of nitrogen-based hemilabile ligands.[21] Hybrid S/N/S ligands consisting of substitutionally inert pyridine moieties and labile sulfur moieties are known.[22–25] In these complexes, the S–S switching, in

---

[a] Dipartimento di Chimica Inorganica, Chimica Analitica e Chimica Fisica, Università di Messina,
Salita Sperone 31, 98166 Vill. S. Agata, Messina, Italy
Fax: +39-090393756
E-mail: tresoldi@chem.unime.it

DOI: 10.1002/ejic.200400976

addition to sulfur inversion, was often observed.[23–25] Although the thioether-containing aromatic nitrogen heterocycles such as di-2-pyridyl sulfide (dps) usually adopts the *N*,*N*-bidentate coordination,[26–32] it can exhibit a variety of bonding modes to a metal, for example, monodentate[29–31] and bridging modes.[30–34] However, the hemilability of dps has been addressed in a few cases, and only the pyridine moieties have been utilized as inert and labile, bound groups.[29–31] Recently we demonstrated that dps, under the proper conditions, binds the ruthenium metal in an *N*,*S*-chelate fashion, leaving one of the rings uncoordinated.[35] In such species some dynamic processes occur, as shown by the temperature dependence of the NMR spectra, but only the restricted uncoordinated ring rotation could be studied and the total dynamic stereochemistry remained unclear.[35] We have been able to obtain activation-energy data for the pyramidal inversion at the coordinated sulfur atom[36] as well as for the restricted rotation of the pendant ring[37] when the ruthenium(II) center is *N*,*S*-chelated by thioether ligands based on pyridine or pyrimidine, and benzyl or phenyl derivatives.

We have now turned our attention to metal complexes that contain unsymmetrical NSN or NSNN thioethers; we are interested in studying the hemilability of these ligands and consequently the interchange process between chemically distinct coordination species. Since the potentially polydentate ligands **L** [**L** = 2-methylpyridyl pyridyl sulfide (**L₁**), 2-methylpyridyl pyrimidyl sulfide (**L₂**) and 2-methylpyridyl 2-(4-methylpyrimidyl) sulfide (**L₃**)] may bind to the ruthenium center through nitrogen atoms[27,28,32,35–37] or nitrogen and sulfur atoms,[35–37] an NMR spectroscopic study has been carried out to identify the different coordination species obtained when **L** reacts with Ru(bipy)$_2$Cl$_2$, Ru(dprs)$_2$Cl$_2$, and Ru(5edprs)$_2$Cl$_2$ and to examine any dynamic process which might lead to their interconversion.

Results

Synthesis of the Compounds

The air-stable compounds **1–9** were obtained by the reactions of *cis*-[RuCl$_2$(*N*,*N*-diimine)$_2$] and **L** as depicted in Scheme 1.

The complexes are yellow or orange solids that are soluble in acetone or acetonitrile. They were characterized by elemental analysis, conductivity measurements in acetonitrile solutions with values characteristic of 1:2 electrolytes (315–350 S cm^2 mol^{-1}), IR spectroscopy, which shows the

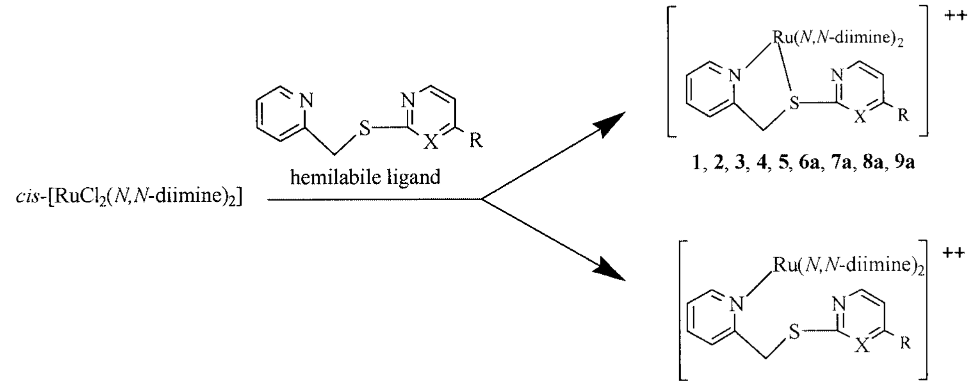

1, **2**, **3**, **4**, **5**, **6a**, **7a**, **8a**, **9a**

6b, **7b**, **8b**, **9b**

cis-[RuCl$_2$(*N*,*N*-diimine)$_2$]	hemilabile ligand	Complex
cis-[Ru(*N*,*N*-bipy)$_2$Cl$_2$]	**L₁** (X = CH, R = H)	**1**
	L₂ (X = N, R = H)	**2**
	L₃ (X = N, R = Me)	**3**
cis-[RuCl$_2$(*N*,*N*-dprs)$_2$]	**L₁**	**4***
cis-[RuCl$_2$(*N*,*N*-5edprs)$_2$]	**L₁**	**5***
cis-[RuCl$_2$(*N*,*N*-dprs)$_2$]	**L₂**	**6a** + **6b**
	L₃	**7a** + **7b**
cis-[RuCl$_2$(*N*,*N*-5edprs)$_2$]	**L₂**	**8a** + **8b**
	L₃	**9a** + **9b**

* At low temperatures only the *N*,*S*-chelated species are observed

Scheme 1.

bands of PF_6^- (ca. 844 and 558 cm^{-1}) and those characteristic of thioether ligands in the range (1630–1540 and 780–720 cm^{-1}). These data indicate that the ligands bipy, dprs, and 5edprs act as *N*,*N*-chelate ligands.[26–32] These findings were confirmed by subsequent ^1H and ^{13}C NMR spectroscopic studies.

Coordination of L$_1$ in [Ru(bipy)$_2$(*N*,*S*/L$_1$)][PF$_6$]$_2$ (1), [Ru(bipy)$_2$(*N*,*S*/L$_2$)][PF$_6$]$_2$ (2), and [Ru(bipy)$_2$(*N*,*S*/L$_3$)][PF$_6$]$_2$ (3).

The crystal structure of [Ru(*N*,*N*-dps)$_2$(*N*,*S*/L$_1$)][PF$_6$]$_2$[37] has shown that **L$_1$** is *N*,*S*-chelated to the ruthenium atom forming the five-membered ring RuSCCN*(Ru–N)*. Further-

Table 1. ^1H NMR spectroscopic data.

Compound[a]	*T*/K	Ring	Positions					*J*(CH$_2$)/Hz	Ring	Positions			
			3	4	5	6	CH$_2$			3	4	5	6
L$_1$	298	A	7.49	7.67	7.19	8.44	4.56		B[b]	7.28	7.59	7.07	8.48
L$_2$	298	A	7.52	7.69	7.21	8.49	4.54		B[c]		8.59	7.15	8.59
L$_3$	298	A	7.52	7.69	7.22	8.49	4.52		B[c]		2.42[d]	7.03	8.42
1	223	A	8.07	7.99	7.22	7.55	5.80	*J* = 16.6	B[b]	6.78	7.37	7.27	8.10
		C	8.32	8.16	7.65	8.31	5.02		D	8.34	8.01	7.45	8.02
		E	8.94	8.36	7.90	9.75			F	8.89	8.23	7.53	7.92
2	298	A	8.07	7.97	7.25	7.59	5.64	*J* = 17.2	B[c]		8.29	7.27	8.29
		C	8.46	8.10	7.47	8.05	5.17		D	8.48	8.07	7.48	7.96
		E	8.85	8.34	7.92	9.64			F	8.80	8.21	7.55	7.87
3	298	A	8.05	7.97	7.25	7.58	5.68	*J* = 17.2	B[c]		2.15[d]	7.13	8.13
		C	8.47	8.11	7.52	8.02	5.15		D	8.51	8.08	7.48	8.08
		E	8.86	8.35	7.92	9.64			F	8.82	8.22	7.55	7.88
4[e]	203	A	7.53	8.01	7.64	9.27	4.55	*J* = 16.9	B[b]	8.15	7.95	7.27	7.55
		C		8.46	7.48	9.33	3.69		D		8.99	7.50	8.84
		E		9.13	7.65	9.06			F		8.94	7.76	9.69
5[e]	228	A	7.50	7.98	7.61	9.36	4.57	*J* = 16.9	B[b]	8.10	7.93	7.26	7.53
		C	1.04[f]	8.41	2.53[g]	9.28	3.83		D	0.87[f]	8.93	2.35[g]	8.78
		E	0.91[f]	9.06	2.40[g]	8.96			F	1.15[f]	8.90	2.58[g]	9.64
6a	218	A	7.55	8.03	7.63	9.22	4.89	*J* = 17.2	B[c]		8.42	7.41	8.42
		C		8.49	7.47	9.28	3.93		D		9.01	7.49	8.84
		E		9.12	7.65	9.05			F		8.94	7.75	9.62
6b[h]	218	A	7.90	8.15	7.63	9.37	5.08	*J* = 15.2	B[c]		8.89	7.70	8.89
							4.18		F		8.66	7.05	7.84
6a + 6b	330	A	7.72	8.05	7.64	9.05	4.99	*J* = 16.4	B[c]		8.51	7.44	8.51
		C		8.98	7.41	8.74	4.01		D		9.05	7.55	8.90
		E		8.82	7.48	8.90			F		8.61	7.40	9.07
7a	215	A	7.55	8.05	7.65	9.23	4.84	*J* = 17.2	B[c]		1.87[d]	7.26	8.44
		C		8.50	7.49	9.29	3.90		D		9.00	7.51	8.86
		E		9.11	7.65	9.06			F		8.95	7.76	9.62
7b[h]	215	A	7.90	8.14	7.60	9.37	5.03	*J* = 15.3	B[c]		2.40[d]	7.70	8.76
		C		8.88			4.14		D		9.10		8.93
		E		9.16	7.71	9.18			F		8.65		7.80
7a + 7b	323	A	7.73	8.06	7.63	9.04	5.00	*J* = 16.7	B[c]		2.18[d]	7.28	8.38
		C		8.98	7.42	8.75	4.03		D		9.04	7.54	8.90
		E		8.82	7.48	8.90			F		8.60	7.40	9.06
8a	228	A	7.51	8.00	7.63	9.33	4.83	*J* = 17.2	B[c]		8.40	7.39	8.40
		C	1.00[f]	8.44	2.60[g]	9.23	3.91		D	0.87[f]	8.94	2.36[g]	8.77
		E	0.90[f]	9.06	2.37[g]	8.97			F	1.14[f]	8.90	2.69[g]	9.57
8b[h]	228	A	7.90	8.10	7.70	9.48	5.11	*J* = 14.9	B[c]		8.98	7.80	8.98
		C	1.08[f]	8.83		9.08	4.22		D				8.81
		E				9.07			F	0.75[f]	8.68		7.73
8a + 8b	328	A	7.65	8.03	7.67	9.18	4.86	*J* = 16.6	B[c]		8.54	7.48	8.54
		C	1.11[f]	8.75	2.52[g]	8.83	3.89		D	0.98[f]	8.80	2.47[g]	8.98
		E	1.03[f]	8.91	2.49[g]	8.54			F	1.09[f]	8.53	2.62[g]	8.96
9a	228	A	7.52	8.01	7.62	9.34	4.76	*J* = 17.2	B[c]		1.89[d]	7.26	8.42
		C	1.04[f]	8.52	2.59[g]	9.23	3.87		D	0.87[f]	8.95	2.35[g]	8.77
		E	0.91[f]	9.06	2.39[g]	8.96			F	1.15[f]	8.91	2.70[g]	9.57
9b[h]	228	A	7.92	8.13	7.71	9.46	5.10	*J* = 14.9	B[c]		2.46[d]	7.69	8.84
		C		8.83		9.08	4.20		D				8.82
		E				9.08			F	0.70[f]	8.68	1.82[g]	7.81
9a + 9b	330	A	7.68	8.04	7.66	9.18	4.84	*J* = 16.6	B[c]		2.23[d]	7.34	8.40
		C	1.09[f]	8.75	2.54[g]	8.85	3.87		D	0.98[f]	8.93	2.47[g]	8.57
		E	1.03[f]	8.81	2.54[g]	8.98			F	1.09[f]	8.55	2.58[g]	8.95

[a] At 300.13 MHz in [D$_6$]acetone, δ in ppm with respect to TMS, coupling constant (Hz). Ring A = picolyl ring in the free and coordinated hemilabile ligands; the coupling constant values are: $J_{6,5} \approx 4.8$, $J_{6,4} \approx 1.9$, $J_{6,3} \approx 0.7$, $J_{5,4} = 7.5$, $J_{5,3} \approx 1.1$, $J_{4,3} \approx 8.0$ (in the free ligands) and $J_{6,5} \approx 5.6$, $J_{6,4} \approx 1.3$, $J_{6,3} \approx 0.7$, $J_{5,4} \approx 7.5$, $J_{5,3} \approx 0.8$, $J_{4,3} \approx 7.8$ (coordinated ligands). Ring C, D, E, and F are pyrimidine rings, $J_{6,5} \approx 6.1$, $J_{6,4} \approx 2.1$, $J_{4,5} \approx 4.6$. [b] S-pyridyl fragment. [c] Pyrimidyl or methylpyrimidyl fragment, $J_{6,5} \approx 4.9$. [d] Methyl of *N*,*S*-ligand. [e] Signal for minor isomer is not observed. [f] Methyl signals of 5edprs. *J* (between methyl and methylene protons) ≈ 7.50. [g] Methylene signals of 5edprs. [h] Minor isomer; only some signals are assigned.

more, in the compounds $[Ru(diimine)_2(N,S/L')][PF_6]_2$ [diimine = dps, 4-mdps, 5-mdps, dprs and 5edprs; **L′** = 2-pyrimidylmethyl *p*-tolyl sulfide and *p*-chlorophenyl 2-pyrimidylmethyl sulfide], **L′** is *N,S*-chelated to Ru and forms a five-membered ring.[37] These data suggest that the present ligands **L** can adopt an *N,S*-coordination in the complexes $Ru(bipy)_2(N,S\text{-}\mathbf{L})][PF_6]_2$. However, the NMR spectra of the complexes $Ru(dprs)_2(N,S\text{-}\mathbf{L})][PF_6]_2$ and $Ru(5edprs)_2(N,S\text{-}\mathbf{L})][PF_6]_2$ (see infra) show the presence of two different coordination species. Thus, in the absence of the crystal structure data of **1**, **2** and **3**, we performed several NMR spectroscopic experiments at various temperatures to exclude the presence of different coordination species.

Identification of the coordination mode of $\mathbf{L_1}$, $\mathbf{L_2}$ and $\mathbf{L_3}$ in compounds **1**, **2** and **3**, respectively, was based preliminarily on the analysis of the ^{1}H NMR spectra. In particular: i) the H(6) and H(4) pyrimidine protons of $\mathbf{L_2}$ in **2** are equivalent in that the pyrimidine ring is uncoordinated, ii) the H(3) signal of the uncoordinated pyridine ring of $\mathbf{L_1}$ appears at an unusually low frequency δ = 6.78 ppm (in the free ligand δ = 7.28 ppm); this upfield shift is consistent with increased shielding as the proton lies above the π cloud of the bipyridine ring C or F in the two invertomers (see infra), iii) the temperature has a negligible effect on the methylene proton signals which appear, at all the temperatures, as a single AB system (for instance in **2** at 223 K, δ = 5.61 and 5.18 ppm, J = 17.3 Hz, and at 330 K, δ = 5.65 and 5.17 ppm, J = 17.2 Hz, see also Table 1). Since **1**, **2** and **3** contain a stereogenic sulfur atom [(*R*) and (*S*) configurations] of the unsymmetrical thioether *N,S*-coordinated ligands and a stereogenic tris-chelated ruthenium center (Δ and Λ configurations), two invertomers are expected as enantiomeric couples (Δ*R*, Λ*S*) and (Δ*S*, Λ*R*). They should give two set of signals in the low-temperature ^{1}H NMR spectra and, in particular, two AB systems for the methylene protons of the two slowly exchanging invertomers. However, the spectra show a single AB system. This can indicate the presence of: 1) only one invertomer, 2) two invertomers that give superimposed signals, 3) two rapidly exchanging invertomers at low temperatures. From literature precedents,[23–25,36] the presence of only one invertomer or two invertomers that have similar resonances is unlikely. Thus, a fast sulfur inversion occurs, even at low temperatures, which is in accordance with the presence of a flexible five-membered chelate ring.[37,38]

On the other hand, the splitting patterns of the methylene protons at higher temperatures (single AB system) rule out the possibility of racemization ($\Delta \rightleftharpoons \Lambda$), which should average the environments of the methylene protons.

The ^{1}H NMR spectra of **1**, **2**, and **3**, in the range 210–330 K (Table 1) show the absence of different coordination species and dynamic processes of interconversion. Furthermore, in the NOESY phase-sensitive experiments of the compounds, positive cross-peaks due to chemical exchange of magnetization are absent.

The NOESY spectrum of **1** at 223 K is shown in Figure 1. Strong NOEs include intraring *ortho* interactions (6–5, 5–4 and 4–3) in the pyridine rings as well as interactions between the methylene protons. Most significantly, it shows interactions between: 1) the H(3) proton of the uncoordinated pyridine ring (labelled B in Table 1) of $\mathbf{L_1}$ at δ = 6.78 ppm, and that of the coordinated pyridine ring (A) at δ = 8.07 ppm; 2) the last proton and the methylene protons at δ = 5.02 and 5.80 ppm, respectively, and the H(6) proton of the bipyridine ligand at δ = 8.31 ppm (ring C); 3) the H(6) bipyridine proton at δ = 9.75 ppm (ring E) and the methylene proton at δ = 5.02 ppm. Weak interactions are observed between the H(3) proton of the uncoordinated pyridine group of $\mathbf{L_1}$ at δ = 6.78 ppm and the methylene proton at δ = 5.80 ppm and the H(6) bipyridine proton at δ = 9.75 ppm (ring E). Furthermore, the NOEs between the H(3) bipyridine protons at δ = 8.32 and 8.34 ppm, and those at δ = 8.94 and 8.89 ppm were used to identify the H(3) protons in the same bipyridine ligand (rings C, D and E, F, respectively).

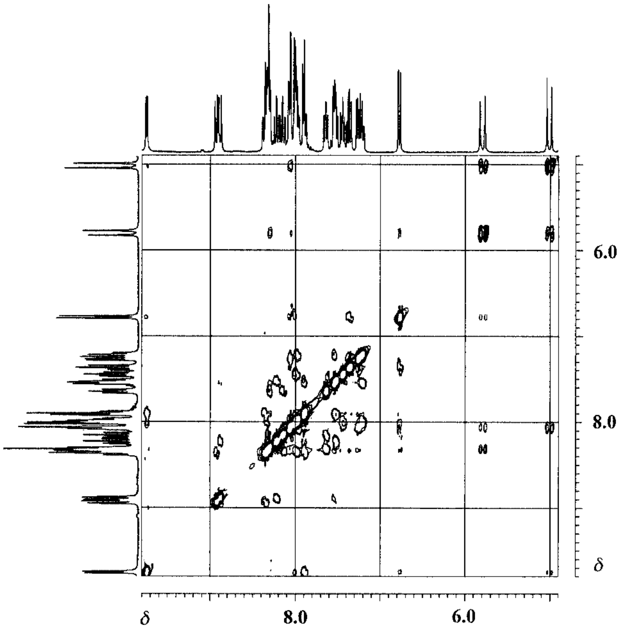

Figure 1. 2D NOESY of $[Ru(bipy)_2L_1][PF_6]_2$ (**1**) at 223 K in [D$_6$]-acetone.

On the basis of 2D phase-sensitive NOESY, 2D COSY, decoupling experiments and monodimensional ^{1}H NMR spectra at various temperatures the *N,S*-coordination of $\mathbf{L_1}$, $\mathbf{L_2}$ and $\mathbf{L_3}$ ligands resulting in the formation of the five-membered ring was assigned. In one invertomer, the uncoordinated pyridine ring B has a *cis* conformation with respect to the pyridine ring labelled C; in the other invertomer, ring B has a *cis* conformation with respect to ring F. Rings and proton positions of **1**, **2** and **3** are listed in Table 1.

Solution Structure of $[Ru(N,N\text{-dprs})_2(N,S/L_1)][PF_6]_2$ (4) and $[Ru(N,N\text{-5edprs})_2(N,S/L_1)][PF_6]_2$ (5) at Low Temperatures

The signal assignments for **4** and **5** were performed with the help of the aforementioned experiments, and the results are listed in Table 1. The portion of the NOESY spectrum of $[Ru(N,N\text{-dprs})_2\mathbf{L_1}][PF_6]_2$ (**4**), performed at 233 K in $(CD_3)_2$-

CO, shown in Figure 2, displays the proton signals of the pyridyl rings labelled A (coordinated ring) and B (uncoordinated ring), the pyrimidyl rings C and D of the same dprs (the first ring is near ring B, Figure 3), and the rings E and F of the other ligand (E is *trans* with respect to the sulfur atom, Figure 3). 6A (δ = 9.27 ppm, $\Delta\delta$ with respect to the free ligand is 0.79 ppm) displays a high-frequency shift due to coordination and short contact with the 6C proton of the pyrimidine ring at δ = 9.33 ppm. The strong NOEs include: a) intraring *ortho* interactions: 6–5, 5–4, and 4–3 in the pyridine rings, 6–5 and 5–4 in the pyrimidine rings; b) geminal interaction of the methylene protons; c) adjacent-group interaction of the methylene proton at δ = 4.55 and 3A at δ = 7.53; d) interaction between the H(6) protons of the pyrimidine rings (6A and 6C, 6F at δ = 9.69 ppm and 6E at δ = 8.84 ppm, 6C and 6D at δ = 9.06 ppm).

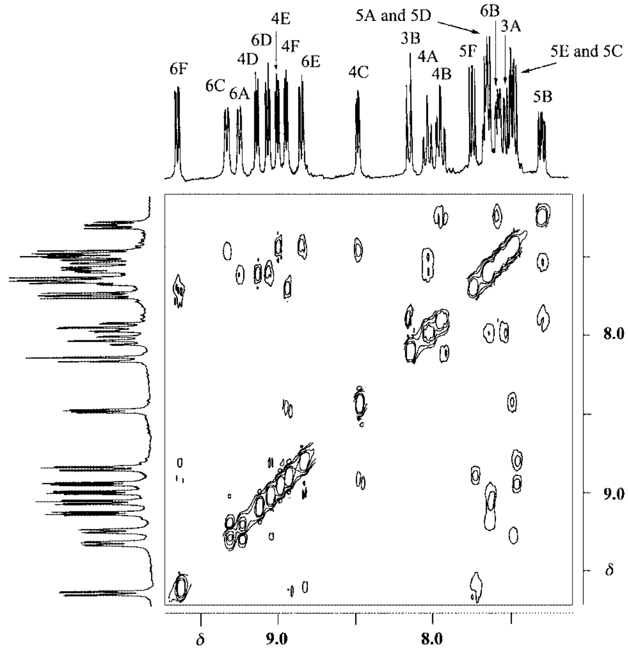

Figure 2. 2D NOESY of $[Ru(dprs)_2L_1][PF_6]_2$ (**4**) at 233 K in $[D_6]$-acetone.

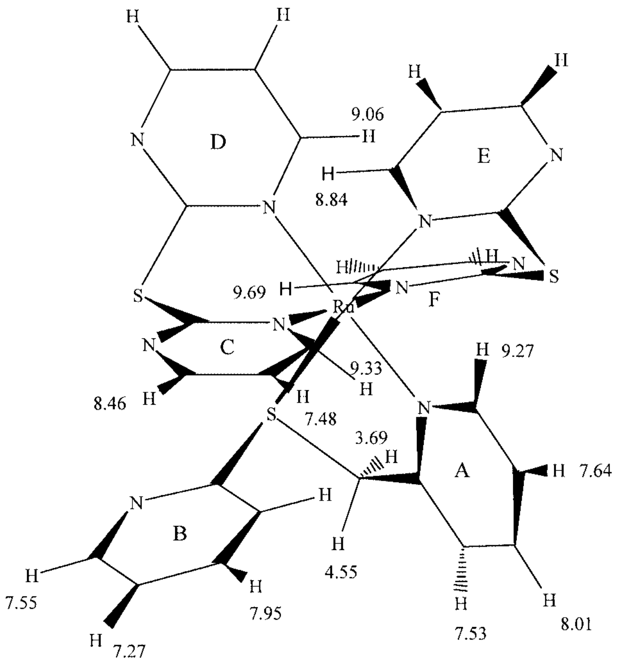

Figure 3. Proposed structure of an invertomer of **4**.

Solution Behaviour of 6a + 6b, 7a + 7b, 8a + 8b and 9a + 9b

Variable-temperature ^1H NMR spectra of the compounds were obtained in $(CD_3)_2CO$ in the range 215–330 K and in CD_3CN (220–370 K). At low temperature in $(CD_3)_2CO$ or CD_3CN, the ^1H NMR spectra of the complexes consist of two sets of signals; one set is much more intense than the other, and this is in agreement with the presence of two different coordination species, one of which was predominant in solution (**6a**, **7a**, **8a**, or **9a**). Identification of these pairs of species was based primarily on the analysis of the proton signals of $\mathbf{L_2}$ or $\mathbf{L_3}$. The shift at high frequencies of the pyridyl proton signals of $\mathbf{L_2}$ and $\mathbf{L_3}$ with respect to the free ligand is in agreement with the pyridyl coordination in both the species. The equivalence, of the pyrimidyl protons 4B and 6B, as well as 4B′ and 6B′ of $\mathbf{L_2}$, suggests that pyrimidyl ring is uncoordinated in both species.

The ^1H NMR spectrum of **6a** + **6b** at 218 K in $(CD_3)_2CO$ is shown in Figure 4. All the proton signals of **6a** and some signals of **6b** are labelled. The data are listed in Table 1. According to the presence of two species (population ratio 87:13), four doublets appear in the methylene region: two doublets of major intensity at δ = 4.89 and 3.93 ppm (J = 17.2 Hz), labelled M and N, respectively, and two doublets at δ = 5.08 and 4.18 ppm (J = 15.2 Hz), labelled M′ and N′, respectively. In the aromatic region, the multiplets of major intensity were all assigned, with the help of NOESY, COSY and decoupling experiments, to the 19 protons of **6a**: 12 nonequivalent pyrimidyl protons of *N,N*-chelated dprs ligands (with the coupling constants $J_{4,5} \approx 4.6$, $J_{4,6} \approx 2.1$, and $J_{5,6} \approx 6.0$ Hz) and seven protons of $\mathbf{L_2}$; of the latter protons, four are pyridyl protons at δ = 7.55 (3A), 8.03 (4A), 7.63 (5A), and 9.22 ppm (6A) and three are pyrimidyl protons (5B at δ = 7.41 ppm and the equivalent 4B and 6B at δ = 8.42 ppm). These signals are clearly associated to the coordination species containing the five-membered ring RuSCCN(*Ru–N*) and the uncoordinated pyrimidyl ring. In the same aromatic region, full assignment of the minor intensity signals was not possible due to their weakness and numerous partial or complete overlap of these signals with the more intense signals. The assignment of some significant signals was made on the basis of the cited experiments and the multiplet structures of these signals which matched those of their major counterparts. In particular, the pyridyl signals of $\mathbf{L_2}$ in **6b** are at δ = 9.37 (6A′), 8.15 (4A′), 7.90 (3A′), and 7.63 ppm (5A′) (the last masked by the signal of the corresponding proton of the major isomer) and the pyrimidyl signals at δ = 7.70 (5B′) and 8.88 ppm (4B′ and 6B′).

The 2D NOESY spectrum of **6a** + **6b** (Figure 5) was obtained at 243 K. At this temperature, some significant signals

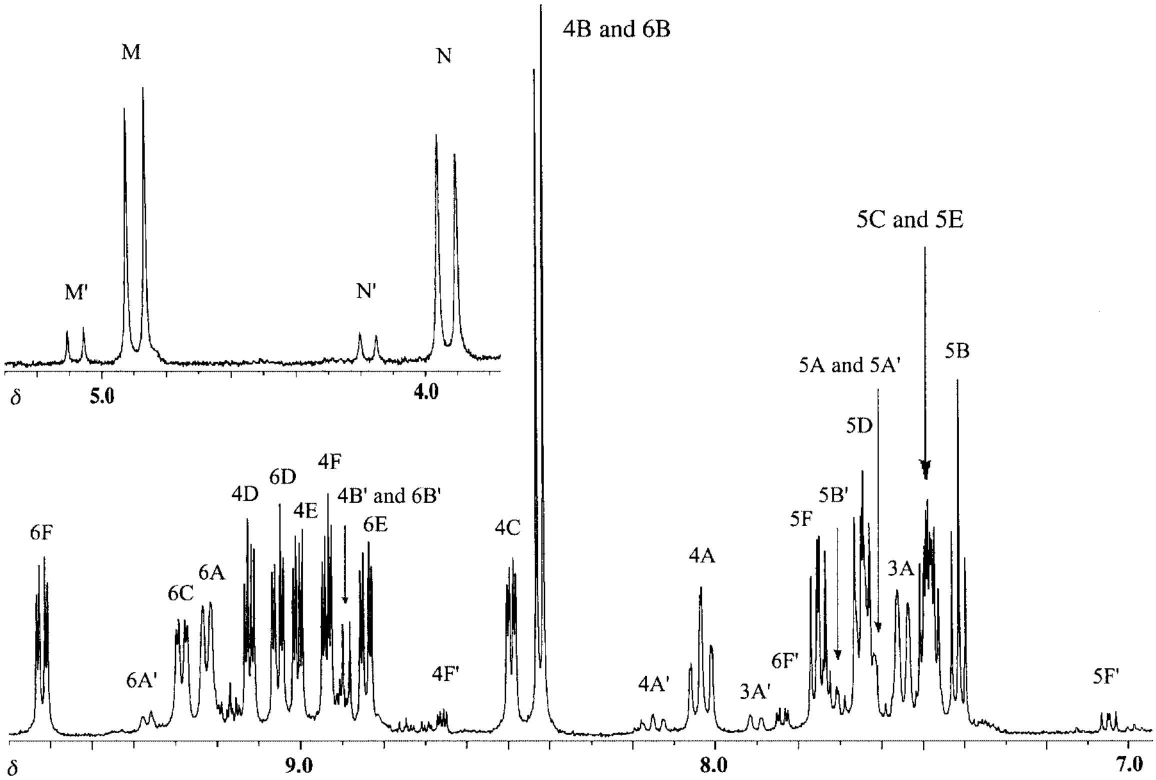

Figure 4. ^{1}H NMR spectrum of $[Ru(dprs)_2L_2][PF_6]_2$ (**6a** + **6b**) at 218 K in [D$_6$]acetone.

of the two species are well separated, and the interchange process is slow. The cross peaks, resulting from chemical exchange of magnetization (grey in Figure 5), are detected in the methylene region between the proton signals M–M′ and N–N′, whereas in the aromatic region (see Figure 4), well-resolved cross peaks are observed between the corresponding **L$_2$** proton signals of the two species (6A – 6A′, 4A – 4A′, 3A – 3A′, 6B and 4B – 6B′ and 4B′, 5B – 5B′) and between 6F (δ = 9.62) and 6F′ (δ = 7.84 ppm), 4F (δ = 8.94 ppm) and 4F′ (δ = 8.66 ppm) and 5F (δ = 7.75 ppm) and 5F′ (δ = 7.05 ppm).

The strong NOEs (black in Figure 5), for the major species, include interactions between the methylene protons, intraring interactions (e.g. 6–5, 5–4 and 4–3 in the pyridine ring and 6–5 and 4 –5 in the pyrimidine rings) and, most significantly, the following interactions between: methylene proton at δ = 4.89 ppm and 3A δ = 7.55 ppm, methylene proton at δ = 3.93 ppm and 6F, equivalent protons (6B and 4B at δ = 8.42 ppm) and 5B at δ = 7.41 ppm.

We assume that the sulfur inversion is fast in the major species even at the low temperatures as observed in **1**, **2**, **3**, **4**, **5**, and similar complexes.[37,38] In fact, the methylene protons of **6a** give only one AB system. On the contrary, if slow inversion occurs at low temperatures, the presence of two diasteroisomers Δ*R* (Λ*S*) and Δ*S* (Λ*R*) should produce two AB systems in the methylene region of the spectrum.[36] There is no restricted rotation of ring B at 218 K. Restricted rotation of the pyrimidine ring probably occurs below this temperature. Unfortunately, experimental difficulties and, in particular, solubility problems ruled out the possibility of performing NMR experiments below 215 K. In terms of fast inversion and rotation, 4B and 6B are equivalent.

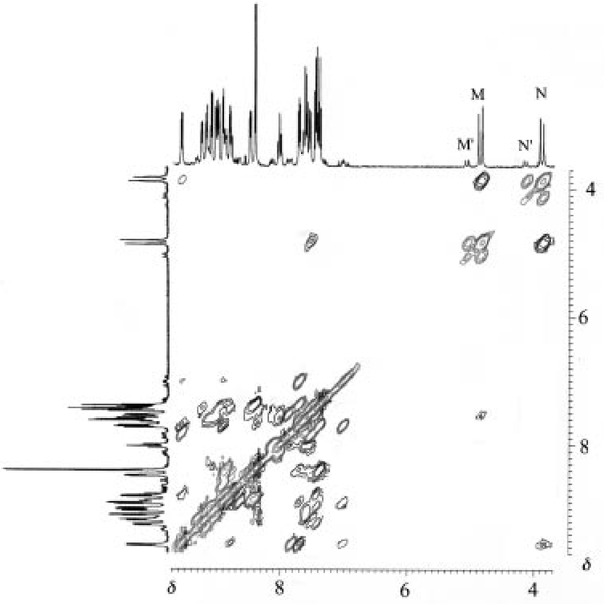

Figure 5. 2D NOESY of $[Ru(dprs)_2L_2][PF_6]_2$ (**6a** + **6b**) at 243 K in [D$_6$]acetone.

The equivalence of 4B′ and 6B′ indicates that the coordination of **L$_2$** does not involve the pyrimidyl group in **6b** also. Since the sulfur inversion and the pyrimidyl rotation are fast, it is unlikely that the minor species is an invertomer or rotamer of the major species. On the other hand, the minor species is very different from the major species. In particular, the coupling constants of the methylene protons in the two species are different (for instance, the coupling constant value in **6a** is 17.2 Hz, whereas in **6b**, 15.2 Hz). Some corresponding signals are very different (the signals of the ring A, B and F with respect to those of rings A′, B′ and F′). Thus, in the minor species, the pyrimidyl coordination as well as the *N,S*-coordination are unlikely. Since the complete dissociation of $\mathbf{L_2}$ or $\mathbf{L_3}$ by the minor species can be excluded because free ligand addition allows for the observation of separate signals for the free and coordinated ligands (Figure 6), the possible species to be considered are the monodentate ones with *N*-(pyridine)- or *S*-coordination. The *N*-coordination is assigned on the basis of: i) the nitrogen of the pyridyl group is a better donor atom than the sulfur atom towards these ruthenium centers;[23,27,28,35–38] ii) the ^{1}H NMR spectra show downfield shifts of the H(6) protons of isomers **6b**, **7b**, **8b**, and **9b** (see Table 1 and 6A′ in Figure 4); iii) the minor species containing the uncoordinated pyrimidine group attached to the sulfur is favored with respect to that containing the pyridine group, whereas a weakening of the Ru–S bond is expected when the pyridine group is replaced by the better electron-withdrawing pyrimidine group.

On warming the solutions, all the spectral lines in the ^{1}H NMR spectra broaden but the signal intensity of the minor species increases. The methylene signals M′ and N′ of **6b** disappear at ca 288 K.

Figure 6 shows the ^{1}H NMR spectrum of **6a** + **6b** in the presence of a small amount of free ligand ($\mathbf{L_2}$) at 330 K, the highest temperature reached. Eighteen signals in the aromatic region and two averaged doublets in the methylene region are observed. Moreover, some signals for free ligand $\mathbf{L_2}$ are observed (in particular, the methylene signal at δ = 4.55 ppm). These NMR findings are in line with the presence of an exchange between the major species containing the five-membered ring RuSCCN(*Ru–N*) and the minor containing the *N*-monodentate ring, in the range 218–330 K. Furthermore, the averaged methylene signals for $\mathbf{L_2}$ at 330 K are observed at δ = 4.99 and 4.01 ppm. These values are the weighted means of 4.89 (M) and 5.08 (M′), and 3.93 (N) and 4.18 (N′) if the population ratio, at this temperature, is 55:45 (see Table 2), whereas at 218 K the ratio is 87:13.

The rates for the process were deduced by band-shape analysis of the methylene signals. Some experimental and computer-simulated spectra of **6a** + **6b** are shown in Figure 7. In the temperature range 218–243 K, the rates are very

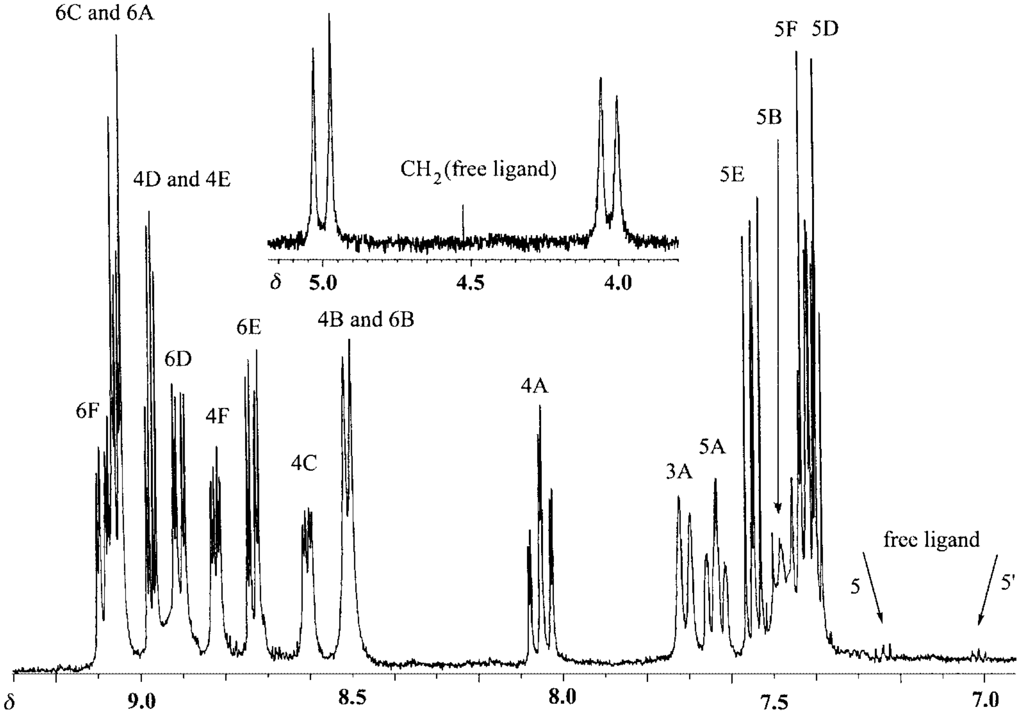

Figure 6. ^{1}H NMR spectrum of $[Ru(dprs)_2L_2][PF_6]_2$ (**6a** + **6b**) at 330 K in [D$_6$]acetone, with small amount of free $\mathbf{L_2}$.

Table 2. Activation energy data.

Species	Population (%) at 218 K	Population (%) at 330 K	$\Delta G^{\#}_{298\,K}$ (kJ·mol^{-1})	$\Delta H^{\#}$ (kJ·mol^{-1})	$\Delta S^{\#}$ (kJ mol^{-1})
6a + **6b**	87:13	55:45	59.1± 0.05	50.5± 1.1	–28.8 ± 3.8
7a + **7b**	82:18	51:49	59.8± 0.10	51.1± 1.3	–29.1 ± 4.8
8a + **8b**	84:16	60:40	59.3± 0.01	57.7± 0.9	–5.4 ± 3.0
9a + **9b**	84:16	60:40	59.5± 0.02	59.0± 1.3	–1.7+4.4

low; however, the population ratio is temperature dependent. To correct for this temperature dependence, a linear interpolation was used.[39] This correction gives the ratio 55:45 at 330 K. Activation parameters were calculated from 15 independent fittings in the temperature range 218–330 K. The activation parameters for the mixtures **7a** + **7b**, **8a** + **8b**, and **9a** + **9b** were obtained in a similar manner and are collected in Table 2.

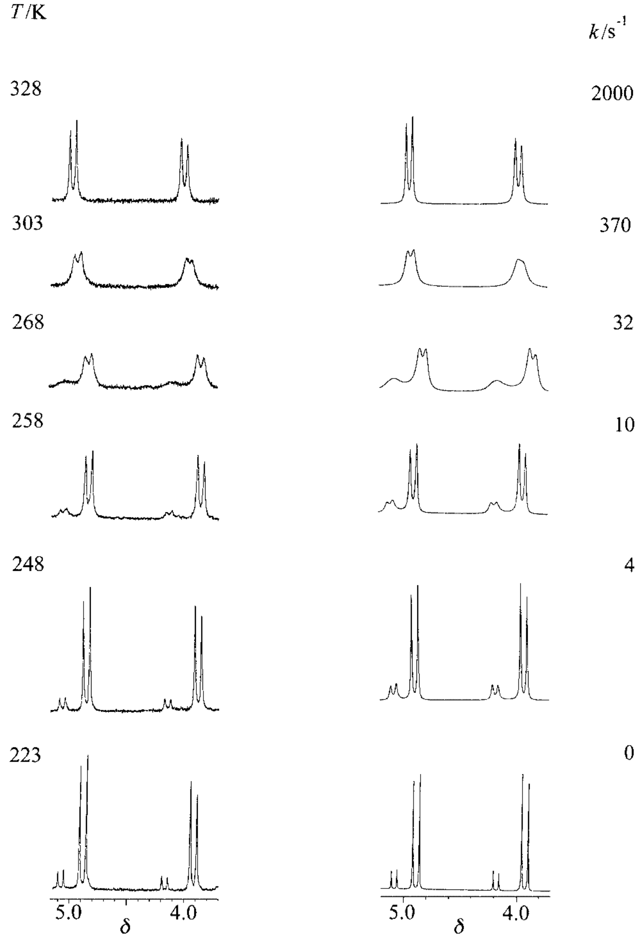

Figure 7. The methylene region of the experimental (left) and computer generated (with the gNMR program, right) ^{1}H NMR spectra of $[Ru(dprs)_2L_2][PF_6]_2$ (**6a** + **6b**) in [D$_6$]acetone.

The ^{13}C NMR spectra of the *N*,*S*-chelate species were interpreted easily (Table 3) by comparison of the spectra of these compounds with those of the free ligand and similar complexes containing *N*,*S*-chelate ligands.[37] Furthermore, although some carbon signals of the minor species are not observed, the ^{13}C NMR spectra show the equivalence of the H(4) and H(6) pyrimidine carbons of **L$_2$** from the presence of uncoordinated pyrimidine ring in the species **6b** and **8b**.

Discussion

We have found that in the complexes [Ru(*N*,*N*-diimine)$_2$(*N*,*S*-pySCH$_2$R)][PF$_6$]$_2$[36] (diimine = dps or dprs, py = pyridine or pyrimidine, and R = phenyl derivative), the ligand pySCH$_2$R is *N*,*S*-coordinated and forms the four-membered ring RuSCN(*Ru–N*). Furthermore, since the ruthenium and sulfur atoms are stereogenic centers, with Δ and Λ, and *R* and *S* configurations, respectively, they lead to the formation of four isomers: Δ*R*, Λ*S*, Λ*R* and Δ*S*. The NMR spectra at various temperatures showed that the pyramidal inversion at the sulfur atom produces an exchange between the diasteroisomers Δ*R* and Λ*S*, as well as between Λ*R* and Δ*S*. The low values of $\Delta G^{\#}_{298}$ (50–55 kJ·mol^{-1}) were explained in terms of the simultaneous presence of the congested Ru(*N*,*N*-dprs)$_2$ fragment and sterically demanding *N*,*S*-coordinated thioethers, which have a high-energy ground state.

In the compounds [Ru(diimine)$_2$(*N*,*S*/L)][PF$_6$]$_2$ [diimine = dps, 4-mdps, 5-mdps, dprs, and 5edprs; L = 2-pyrimidylmethyl *p*-tolyl sulfide (**a**) and *p*-chlorophenyl 2-pyrimidylmethyl sulfide (**b**)], **a** and **b** are *N*,*S*-chelated and form a five-membered ring RuSCCN(*Ru–N*). A restricted phenyl rotation, which exchanges *ortho* as well as *meta* phenyl protons, was also observed. The values of $\Delta G^{\#}_{298}$ are 49–55 kJ·mol^{-1}.

In the present compounds **1**, **2** and **3**, the ligands 2-pyridylmethyl 2′-pyridyl sulfide (**L$_1$**), 2-pyridylmethyl 2′-pyrimidyl sulfide (**L$_2$**), and 2-pyridylmethyl 2′-(4-methylpyrimidyl) sulfide (**L$_3$**) adopt only the *N*,*S*-coordination and form five-membered rings RuSCCN(*Ru–N*) as observed in the crystal structure of [Ru(dps)$_2$(2-pyridylmethyl 2′-pyridyl sulfide)][PF$_6$]$_2$.[37]

The expected invertomers Δ*R* and Λ*S*, and Δ*S* and Λ*R* give only one set of signals in the ^{1}H NMR spectra even at low temperatures as a result of fast sulfur inversion. For the complexes **4–9**, two fast exchanging *N*,*S*-chelated invertomers are present, as observed in similar species containing flexible five-membered *N*,*S*-chelated ring.[37]

Although the NMR spectra at low temperatures of **4** and **5** are in agreement with *N*,*S*-coordination, in the range 290–310 K, the proton signals broaden, particularly, the H(6) signal of the dprs ring F. These NMR findings are likely to be associated with the presence of the *N*-monodentate species at high temperature. It is pertinent to note at this point that a strong temperature dependence of the population ratio is normally observed in these systems (see population ratio of **6a** + **6b**, **7a** + **7b**, **8a** + **8b** and **9a** + **9b** in Table 2). Furthermore, very different resonances are observed for corresponding protons 6F and 6F′ of the two different coordination species (Table 1). In other words, at low temperature the *N*,*S*-chelated species of **4** and **5** largely predominates, the concentration of the *N*-monodentate species increases on warming; the H(6) signals of ring F are sensitive to this process.

For **4** and **5**, we cannot calculate the activation parameters of the process, as we do not know the population ratio and difference in the chemical shifts of the two species at low temperatures.

With regard to a mechanism that is consistent with the exchange of the two different coordination species (**6a** + **6b**, **7a** + **7b**, **8a** + **8b** and **9a** + **9b**), we base our suggestion preliminarily on the following observations: i) The $\Delta G^{\#}_{298}$ values for these mixtures are almost the same, approximately equal to 59,5 kJ·mol^{-1}; ii) the $\Delta S^{\#}$ values are negative for **6a** + **6b** and **7a** + **7b** and close to zero for **8a** + **8b** and **9a** + **9b**.

Table 3. ^{13}C NMR spectroscopic data.

Complex[a]	Asymmetric thioether ligand						Other ligands				
T [K]	C(2)	C(3)	C(4)	C(5)	C(6)	CH$_2$	C(2)	C(3)	C(4)	C(5)	C(6)
L$_1$	158.8[b]	123.4[b]	136.9[b]	122.1[b]	149.8[b]	36.0[b]	158.8[c]	122.4[c]	136.7[c]	120.1[c]	149.6[c]
L$_2$	158.1[b]	123.3[b]	136.8[b]	122.4[b]	149.6[b]	36.8[b]	171.7[d]		157.8[d]	117.4[d]	157.8[d]
L$_3$	158.7[b]	123.6[b]	137.0[b]	122.6[b]	149.9[b]	37.1[b]	171.4[d]	23.7[e]	168.3[d]	117.0[d]	157.6[d]
1	162.8[b]	128.4[b]	139.3[b]	125.4[b]	153.4[b]	39.4[b]	157.2	125.6	138.4	124.2	151.6
	148.4[c]	125.5[c]	138.4[c]	123.9[c]	150.9[c]		157.3	127.7	138.5	124.3	152.0
							157.6	128.3	138.6	124.4	152.6
							158.1	128.4	139.1	125.3	152.9
2	162.9[b]	128.9[b]	138.7[b]	125.5[b]	151.8[b]	41.4[b]	157.7	125.6	138.7	124.4	152.2
	171.6[d]		159.4[d]	120.9[d]	159.4[d]		157.8	125.9	138.8	124.5	152.3
							158.0	127.7	139.3	125.3	153.0
							158.2	128.4	139.5	125.4	153.9
3	163.2[b]	129.0[b]	138.7[b]	125.7[b]	151.9[b]	41.4[b]	157.9	125.9	138.8	124.4	152.3
	170.4[e]	23.4[d]		120.6[e]	158.5[e]		157.9	127.8	138.9	124.5	152.5
							158.1	128.4	139.4	125.5	153.2
							158.3	128.9	139.6	125.6	153.9
4[h]	163.0[b]	129.6[b]	138.3[b]	123.4[b]	154.8[b]	44.3[b]	168.7		156.9	121.6	164.1
233	151.5[c]	124.8[c]	138.1[c]	120.2[c]	149.2[c]		169.5		158.4	121.7	164.8
							169.6		158.4	122.3	164.9
							169.7		158.8	123.1	165.0
5[h]	165.4[b]	126.5[b]	139.9[b]	125.2[b]	157.1[b]	46.8[b]	166.9	15.5[f]	158.5	138.8	163.6
325	153.7[c]		140.0[c]	125.0[c]	151.0[c]		167.4	15.7[f]	159.8	139.8	165.1
		23.6[g]	23.5[g]	23.4[g]	23.3[g]		169.3	16.0[f]	159.8	140.1	165.2
							169.8	16.1[f]	160.5	140.7	165.2
6a	163.5[b]	124.1[b]	138.7[b]	123.9[b]	155.3[b]	44.1[b]	169.3		157.6	122.0	164.6
243	172.3[d]		158.9[d]	120.8[d]	158.9[d]		170.1		159.0	122.1	165.5
							170.2		159.0	122.3	165.5
							170.7		159.4	122.9	165.9
6b[i]			139.0[b]			44.4[b]	169.1[j]	170.4[j]	158.0[k]		158.2[k]
243			159.8[d]	121.1[d]	159.8[d]		169.4[j]	170.4[j]	158.0[k]		158.2[k]
6a + **6b**	164.4[b]	125.9[b]	140.2[b]	125.8[b]	156.9[b]	45.4[b]	170.8		159.9	122.9	166.4
325			160.2[d]	122.2[d]	160.2[d]		170.8		160.1	123.0	166.5
							172.0		160.5	123.1	166.6
							172.0		160.9	124.0	166.7
7a	163.3[b]	123.8[b]	138.3[b]	123.7[b]	155.0[b]	43.9[b]	169.1		157.3	121.0	164.8
243	172.5[d]	22.5[e]	161.7[d]	120.3[d]	159.1[d]		169.9		158.1	121.9	165.2
							170.0		158.7	122.1	165.3
							170.7		158.7	122.6	165.3
7b[i]	163.1[b]	124.8[b]	139.3[b]	124.4[b]	155.9[b]	43.7[b]	168.8[j]	169.5[j]		165.0[l]	165.1[l]
243		23.1[e]		120.7[d]	159.6[d]		170.2[j]	170.8[j]		165.7[l]	166.0[l]
7a + **7b**		125.9[b]	140.1[b]	125.8[b]	156.7[b]	45.2[b]	170.7		159.2	122.3	164.7
323	172.5[d]	23.9[e]		122.0[d]	160.7[d]		171.3		159.5	123.0	166.3
							171.9		159.8	123.1	166.5
							172.0		160.0	124.0	166.5
8a		124.5[b]	139.1[b]	124.0[b]	155.8[b]	44.3[b]	169.0	15.1[f]	158.0	137.8	164.7
243			158.8[d]	121.3[d]	158.8[d]		169.2	15.2[f]	158.1	137.9	165.0
							160.9	15.3[f]	158.5	138.2	165.5
							170.1	15.6[f]	158.7	138.6	166.0
8b[i]		125.0[b]	139.9[b]	124.9[b]	156.8[b]	44.0[b]	168.9[j]	169.5[j]			
243			159.8[d]	121.8[d]	159.8[d]		170.0[j]	170.6[j]			
8a + **8b**		125.6[b]	140.3[b]	125.6[b]	157.4[b]	45.9[b]	168.1	15.4[f]	159.3	139.0	163.4
325			160.3[d]	123.1[d]	160.3[d]		169.8	15.7[f]	159.8	139.5	165.1
		23.6[g]	23.5[g]	23.3[g]	23.3[g]		169.9	15.9[f]	159.9	140.1	165.3
							170.2	16.1[f]	160.7	140.8	165.5
9a	163.9[b]	123.5[b]	138.0[b]	122.9[b]	155.1[b]	43.6[b]		15.1[f]	157.7	136.6	164.7
233		22.4[e]	162.1[d]	120.8[d]	158.6[d]			15.2[f]	157.8	138.4	165.2
		22.0[g]	21.8[g]	21.8[g]	21.6[g]			15.2[f]	158.2	138.5	167.3
								15.6[f]	158.3	139.0	168.6
9b[i]	163.9[b]	122.5[b]	139.1[b]	123.7[b]	156.7[b]	42.3[b]			164.3[l]	136.3	166.2[l]
233		23.4[e]	162.1[d]	120.9[d]	159.3[d]						168.0[l]
9a + **9b**	164.8[b]	125.7[b]	140.2[b]	125.5[b]	157.3[b]	45.8[b]		15.4[f]	158.9	138.7	163.3
325		24.1[e]	164.2[d]	122.4[d]	160.7[d]			15.7[f]	159.5	139.5	165.1
		23.6[b]	23.5[g]	23.4[g]	23.3[g]			15.7[f]	159.7	140.0	165.3
								16.1[f]	159.8	140.8	165.5

[a] Recorded at 75.56 MHz in [D$_6$]acetone and 298 K unless stated otherwise. [b] CH$_2$-pyridyl fragment. [c] S-pyridyl fragment. [d] Pyrimidyl fragment. [e] Methyl signal of **L$_3$**. [f] Methyl signal of 5edprs. [g] Methylene signal of 5edprs. [h] The signals for the minor isomer is not observed. [i] Minor isomer, only a few signals are assigned. [j] C(2) signal of dprs or 5edprs. [k] C(4) signal of dprs. [l] C(6) signal of dprs.

We propose that the mechanism for the interconversion involves the formation of a labile *N*,*N*-intermediate, and subsequent fast dissociation of the Ru–N(pyrimidine) bond, which gives rise to the *N*-monodentate species (Scheme 2). The hemilabile ligands $\mathbf{L_2}$ or $\mathbf{L_3}$ contain three different types of bonding groups. The pyridine group bonds strongly to a metal center, whereas the sulfur and the pyrimidine nitrogen atoms are substitutionally labile groups. In other words, the ruthenium atom undergoes a 1,3-shift between the N(pyrimidine) atom and the sulfur atom, whereas the N(pyridine) atom is always coordinated to the metal, as a result of the ligand attempting, but failing, to adopt a terdentate bonding. The labile *N*,*N*-intermediate involves a seven-coordinate metal transition-state in which S and N(pyrimidine) atom contribute to the bonding. Furthermore, as a consequence of the rotation of the pyrimidine ring in the *N*,*S*-chelate and the *N*-monodentate species, involvement of the both N(pyrimidine) atoms in the coordination is achieved. A substantially stronger Ru–N(pyridine) bond than the Ru–S and Ru–N(pyrimidine) bonds would favor this mechanism.

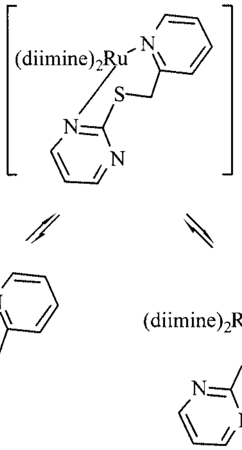

Scheme 2. Proposed mechanism of the interconversion between the different coordination species.

The negative or close to zero $\Delta S^{\#}$ values reflect the formation of a seven-coordinate metal transition-state, while the $\Delta G^{\#}_{298}$ values, practically unchanged by substitution of $\mathbf{L_2}$ with $\mathbf{L_3}$, are compatible with the a similar congested nature of the transition state in all the complexes.

A simple dissociative mechanism involving rupture of the Ru–S bond in the *N*,*S*-chelated species is unlikely, not only because the $\Delta S^{\#}$ values are negative or close to zero, but also because of the following NMR findings: 1) the ^{1}H NMR signals are temperature-reversible and concentration-independent; 2) the process is clearly the same in acetone and acetonitrile below 345 K (in acetonitrile above this temperature some decomposition is observed); 3) the substitution of the uncoordinated pyridine ring with the pyrimidine ring favors the dynamic process.

Although electronic effects can be invoked to explain this behavior, these effects are not observed when the H(4) pyrimidyl proton of $\mathbf{L_2}$ is substituted with the methyl group or when the H(5) pyrimidyl proton of dprs is substituted with the ethyl group.

It is important to note at this point that the process is present only in congested ruthenium cores in which the *N*,*S*-chelated ligand must contain at least three donor atoms, and is favored by the presence of two donor atoms in the uncoordinated pyrimidine ring. The pyrimidine group bonded to the sulfur atom not only weakens the Ru–S bond but also increases the statistical probability of the *N*,*N*-intermediate.

On the other hand, an associative mechanism, involving solvent, anion, or free ligand, is incompatible with the following observations: a) addition of free ligand or PF_6^- anion does not affect the rates of the process; b) separate signals for the free and coordinated ligand were observed in the range 200–330 K (Figure 6). Therefore, the mechanism, consistent with the experimental results, appears to involve the labile *N*,*N*-chelated intermediate.

Conclusions

The reactions of thioethers bearing CH_2Py and pyridine or pyrimidine groups with $Ru(dprs)_2Cl_2$ has allowed us to extend the chemistry of octahedral congested ruthenium(II) compounds containing *N*,*S*-chelated ligands with a five-membered chelate ring. The ring size of *N*,*S*-chelated ligands plays a determining role for sulfur inversion. In the five-membered chelate ring, the process is fast, in the four-membered ring, it is much slower.[36] The NMR experiments show that a minor species containing the *N*-monodentate thioether is favored by the presence of two nitrogen atoms in the uncoordinated ring, whereas it is not observed when the nitrogen atoms are absent.[37] Further experiments are in progress with the aim of studying the effect of the nature of congested Ru(*N*,*N*-dimmine)$_2$ cores on the interconversion between different coordination species.

Experimental Section

General Remarks: Bis(2-pyrimidyl) sulfide,[35] 2-pyridylmethyl 2′-pyridyl sulfide ($\mathbf{L_1}$),[40] 2,2′-bis(5-ethylpyrimidyl) sulfide (5edprs),[37] [Ru(dprs)$_2$Cl$_2$]·2 H$_2$O,[35] and [Ru(5edprs)$_2$Cl$_2$][37] were prepared according to published methods. Ru(bipy)$_2$Cl$_2$ and other reagents and solvents were used as received. All the syntheses were performed under N_2, and all the complexes were dried over P_4O_{10} under vacuum. Elemental analyses were carried out by Redox Microanalytical Laboratory of Cologno Monzese (Milano). Conductivity measurements were done on a Metrohm 644 conductometer. Infrared spectra were recorded with a Perkin–Elmer RX I FT-IR spectrophotometer with samples as Nujol mulls placed between KBr plates, and the ^{1}H and ^{13}C NMR spectra were recorded with a Bruker AMX 300 spectrometer. Simulations of static and dynamic spectra were performed by the gNMR program.

Preparations

The known[40] 2-pyridylmethyl 2′-pyrimidyl sulfide ($\mathbf{L_2}$) was prepared with the following procedure: 2-sulfanylpyrimidine (5.6 g, 0.05 mol), 2-picolyl chloride hydrochloride (8.2 g, 0.05 mol), and K_2CO_3

(9.67 g, 0.07 mol) were vigorously stirred in DMF (30 cm^3) at 100 °C for 6 h. The solvent was distilled under reduced pressure, and the residue extracted with CH_2Cl_2 (200 cm^3). This was then concentrated (ca. 5 cm^3) and added to the top of the chromatography column (diameter 2 cm) packed with aluminium oxide (35 g; Aldrich neutral, STD grade, 150 mesh). Elution with CH_2Cl_2/hexane (5:2) gave a pale yellow band, which was collected. The solvent was removed in vacuo, and the remaining yellow oil was kept at –24 °C until a solid was formed (ca. 2 d). Yield 4.57 g (45%). Selected IR data (KBr): $\tilde{\nu}$ = 1670 vs, 1590 vs, 1563 vs, 1548 vs, 1257 s, 1199 vs, 1184 vs, 1091 vs, 994 s, 799 vs, 773 vs, 749 vs, 734 s and 588 ms cm^{-1}.

2-Pyridylmethyl 2′-(4-Methylpyrimidyl) Sulfide (L_3): Prepared similarly starting from 2-mercapto-4-methylpyrimidine hydrochloride (8.13 g, 0.05 mol), 2-picolyl chloride hydrochloride (8.20 g, 0.05 mol), and K_2CO_3 (16.7 g, 0.12 mol). Yield 4.35 g (40%). Selected IR data (KBr): $\tilde{\nu}$ = 1592 vs, 1568 vs, 1541 vs, 1223 s, 1206 vs, 1091 s, 995 s, 881 s, 785 s, 771 s, 750 vs, 713 vs, 698 s, 590 s, 547 s and 406 s cm^{-1}. $C_{11}H_{11}N_3S$ (217.29), calcd. C 60.80, H 5.10, N 19.34, S 14.75; found C 60.70, H 5.20, N 19.50, S 14.70.

$[Ru(bipy)_2(L_1)][PF_6]_2$ (1): $[Ru(bipy)_2Cl_2]\cdot 2H_2O$ (0.174 g, 0.33 mmol) in degassed ethanol/water (3:2, 50 cm^3) was heated under reflux for 1 h. 2-pyridylmethyl 2′-pyridyl sulfide (0.178 g, 0.882 mmol) was then added, and the mixture was heated under reflux for a further 4 h. The hot solution was filtered, and the filtrate was added to water (50 cm^3) containing NH_4PF_6 (0.98 g, 6.0 mmol). An orange precipitate was obtained, filtered, washed with water, and dried overnight. The solid was dissolved in acetone (15 cm^3), precipitated with diethyl ether (100 cm^3), and washed with diethyl ether (70 cm^3). Yield 0.181 g (60%). Selected IR data (KBr): $\tilde{\nu}$ = 1605 s, 1575 s, 1560 ms, 1548 ms, 1515 s, 1315 s, 1243 s, 1162 s, 1125 s, 845 br, 764 vs, 740 ms, 730 s, 558 vs cm^{-1}. $C_{31}H_{26}F_{12}N_6P_2RuS$ (905.65), calcd. C 41.11, H 2.89, N 9.28, S, 3.54; found: C 40.90, H 3.00, N 9.30, S 3.60. Conductivity: Λ_M (MeCN, 2×10^{-4} $mol\cdot dm^{-3}$, 20 °C) = 333 $S\cdot cm^2\cdot mol^{-1}$.

$[Ru(bipy)_2(L_2)][PF_6]_2$ (2): This compound was obtained in the same way as that described above starting from $[Ru(bipy)_2Cl_2]\cdot 2H_2O$ (0.302 g, 0.623 mmol) and 2-pyridylmethyl 2′-pyrimidyl sulfide (0.630 g, 3.100 mmol). Yield 0.339 g (60%). Selected IR data (KBr): $\tilde{\nu}$ = 1605 s, 1561 s, 1557 vs, 1315 ms, 1243 ms, 1164 s, 1108 s, 838 br, 764 vs, 731 s, 558 vs cm^{-1}. $C_{30}H_{25}F_{12}N_7P_2RuS$ (906.64), calcd. C 39.74, H 2.78, N 10.81, S, 3.53; found: C 39.70, H 2.80, N 10.85, S 3.60. Conductivity: Λ_M (MeCN, 2×10^{-4} $mol\cdot dm^{-3}$, 25 °C) = 310 $S\cdot cm^2\cdot mol^{-1}$.

$[Ru(bipy)_2(L_3)][PF_6]_2$ (3): The compound was obtained in the same way as that described above starting from $[Ru(bipy)_2Cl_2]\cdot 2H_2O$ (0.200 g, 0.413 mmol) and 2-pyridylmethyl 2′-(4-methylpyrimidyl) sulfide (0.510 g, 2.34 mmol). Yield 247 (65%). Selected IR data (KBr): $\tilde{\nu}$ = 1603 ms, 1575 s, 1534 ms, 1163 ms, 844 br, 768 vs, 732 ms, 558 vs cm^{-1}. $C_{31}H_{27}F_{12}N_7P_2RuS$ (920.66), calcd. C 40.44, H 2.95, N 10.65, S, 3.48; found: C 40.40, H 2.90, N 10.65, S 3.50. Conductivity: Λ_M (MeCN, 2×10^{-4} $mol\cdot dm^{-3}$, 25 °C) = 340 $S\cdot cm^2\cdot mol^{-1}$.

$[Ru(dprs)_2(L_1)][PF_6]_2$ (4): $[Ru(dprs)_2Cl_2]\cdot 2H_2O$ (0.196 g, 0.33 mmol) and 2-pyridylmethyl 2′-pyridyl sulfide (0.178 g, 0.882 mmol) in ethanol/water (3:2, 50 cm^3) were heated under reflux under N_2 for 4 h. The hot solution was filtered, and the filtrate was added to water (50 cm^3) containing NH_4PF_6 (0.65 g, 4 mmol). An orange precipitate was obtained, filtered, washed with cold water (30 cm^3), and dried overnight. The solid was then dissolved in acetone (15 cm^3), precipitated with diethyl ether (100 cm^3), washed with diethyl ether (70 cm^3), and dried over P_4O_{10} under vacuum. Yield 0.195 g (60%). Selected IR data (KBr): $\tilde{\nu}$ = 1654 br, 1575 s, 1549 s, 1168 s, 1127 s, 1085 ms, 847 br, 767 s, 753 s, 721 ms, 559 vs cm^{-1}. $C_{27}H_{22}F_{12}N_{10}P_2RuS_3$ (973.72), calcd. C 33.31, H 2.28, N 14.38, S, 9.88; found: C 33.30, H 2.30, N 14.20, S 9.80. Conductivity: Λ_M (MeCN, $2\cdot10^{-4}$ $mol\cdot dm^{-3}$, 25 °C) = 320 $S\cdot cm^2\cdot mol^{-1}$.

$[Ru(5edprs)_2(L_1)][PF_6]_2$ (5): The compound was obtained in the same way as **4** starting from $[Ru(5edprs)_2Cl_2]$ (0.219 g, 0.33 mmol) and 2-pyridylmethyl 2′-pyridyl sulfide (0.178 g, 0.882 mmol). Yield 0.215 g (60%). Selected IR data (KBr): $\tilde{\nu}$ = 1653 br, 1574 s, 1548 vs, 1242 s, 1145 vs, 1061 vs, 878 vs, 845 br, 780 s, 765 s, 721 ms, 558 vs cm^{-1}. $C_{35}H_{38}F_{12}N_{10}P_2RuS_3$ (1085.93), calcd. C 38.71, H 3.53, N 12.90, S, 8.86; found: C 38.60, H 3.60, N 12.80, S 8.80. Conductivity: Λ_M (MeCN, $2\cdot10^{-4}$ $mol\cdot dm^{-3}$, 25 °C) = 315 $S\cdot cm^2\cdot mol^{-1}$.

$[Ru(dprs)_2(L_2)][PF_6]_2$ (6a + 6b): The procedure used in this synthesis was similar to that described for **4** starting from $[Ru(dprs)_2Cl_2]\cdot 2H_2O$ (0.196 g, 0.33 mmol) and 2-pyridylmethyl 2′-pyrimidyl sulfide (0.178 g, 0.882 mmol.) Yield 0.195 g (60%). Selected IR data (KBr): $\tilde{\nu}$ = 1654 br, 1578 vs, 1561 s, 1549 vs, 1169 vs, 1085 s, 845 br, 769 ms, 754 s, 723 ms, 558 vs cm^{-1}. $C_{26}H_{21}F_{12}N_{11}P_2RuS_3$ (974.71), calcd. C 32.04, H 2.17, N 15.81, S 9.87; found C 32.00, H 2.20, N 15.60, S 9.80. Conductivity: Λ_M (MeCN, $2\cdot10^{-4}$ $mol\cdot dm^{-3}$, 25 °C) = 318 $S\cdot cm^2\cdot mol^{-1}$.

$[Ru(dprs)_2(L_3)][PF_6]_2$ (7a + 7b): The procedure used in this synthesis was similar to that described above with an equivalent quantity of 2-pyridylmethyl 2′-(4-methylpyrimidyl) sulfide (0.192 g, 0.882 mmol) used in place of $\mathbf{L_2}$. Yield 0.190 g (68%). Selected IR data (KBr): $\tilde{\nu}$ = 1575 vs, 1549 vs, 1261 s, 1167 vs, 1086 s, 846 br, 767 ms, 753 s, 721 ms, 558 vs cm^{-1}. $C_{27}H_{23}F_{12}N_{11}P_2RuS_3$ (988.74), calcd. C 32.80, H 2.34, N 15.58, S 9.73; found C 32.60, H 2.40, N 15.60, S 9.80. Conductivity: Λ_M (MeCN, $2\cdot10^{-4}$ $mol\cdot dm^{-3}$, 25 °C) = 321 $S\cdot cm^2\cdot mol^{-1}$.

$[Ru(5edprs)_2(L_2)][PF_6]_2$ (8a + 8b): $[Ru(5edprs)_2Cl_2]$ (0.219 g, 0.33 mmol) and 2-pyridylmethyl 2′-pyrimidyl sulfide (0.178 g, 0.882 mmol) in ethanol/water (3:2, 50 cm^3) were heated under reflux for 2 h. $AgPF_6$ (0.167 g 0.66 mmol) was then added, and the mixture was stirred for 1 h at 50 °C in the dark. After filtration of the solution into water (50 cm^3) containing NH_4PF_6 (0.65 g, 4.0 mmol), an orange precipitate was obtained, filtered, washed with cold water (30 cm^3), and dried overnight. Aluminium oxide (0.200 g) was added to the crude product dissolved in acetone (15 cm^3), and the mixture was stirred for 15 min. The solution was then filtered, and the aluminium oxide was washed with acetone (5 cm^3). The solution and washing liquids were concentrated (5 cm^3), and diethyl ether (50 cm^3) was added. The precipitate was collected and washed with diethyl ether. Yield 0.108 g (30%). Selected IR data (KBr): $\tilde{\nu}$ = 1580 s, 1556 s, 1549 vs, 1260 vs, 1093 vs, 1061 s, 1022 vs, 845 br, 777 s, 754 s, 740 ms, 721 s, 558 vs cm^{-1}. $C_{34}H_{37}F_{12}N_{11}P_2RuS_3$ (1086.93), calcd. C 37.57, H 3.43, N 14.18, S 8.85; found C 37.60, H 3.55, N 14.10, S 8.80. Conductivity: Λ_M (MeCN, $2\cdot10^{-4}$ $mol\cdot dm^{-3}$, 25 °C) = 343 $S\cdot cm^2\cdot mol^{-1}$.

$[Ru(5edprs)_2(L_3)][PF_6]_2$ (9a + 9b): The procedure used in this synthesis was similar to that described above with an equivalent quantity of 2-pyridylmethyl 2′-(4-methylpyrimidyl) sulfide (0.192 g, 0.882 mmol) used in place of $\mathbf{L_2}$. Yield 0.134 g (37%). Selected IR data (KBr): $\tilde{\nu}$ = 1575 vs, 1548 vs, 1143 s, 1061 s, 841 br, 757 s, 740 ms, 721 ms, 558 vs cm^{-1}. $C_{35}H_{39}F_{12}N_{11}P_2RuS_3$ (1100.95), calcd. C 38.18, H 3.57, N 13.99, S 8.74; found C 38.20, H 3.60, N 13.90, S 8.80. Conductivity: Λ_M (MeCN, $2\cdot10^{-4}$ $mol\cdot dm^{-3}$, 25 °C) = 350 $S\cdot cm^2\cdot mol^{-1}$.

Acknowledgments

This work was supported by the Università di Messina, Italy (PRA, 2002).

---

[1] C. S. Slone, D. A. Weimberg, C. A. Mirkin, *Prog. Inorg. Chem.* **1999**, *48*, 233–350.

[2] E. W. Abel, N. J. Long, K. G. Orrell, A. G. Osborne, H. M. Pain, V. Sik, *J. Chem. Soc. Chem. Commun.* **1992**, 303–304.

[3] E. W. Abel, V. S. Dimitrov, N. J. Long, K. G. Orrell, A. G. Osborne, V. Sik, M. B. Hursthouse, M. A. Mazid, *J. Chem. Soc. Dalton Trans.* **1993**, 291–298.

[4] E. W. Abel, K. A. Hylands, M. D. Olsen, K. G. Orrel, A. G. Osborne, W. Sik, G. N. Ward, *J. Chem. Soc. Dalton Trans.* **1994**, 1079–1090.

[5] E. W. Abel, A. Gelling, K. G. Orrell, A. G. Osborne, V. Sik, *J. Chem. Soc. Chem. Commun.* **1996**, 2329–2330.

[6] P. J. Heard, D. A. Tocher, *J. Chem. Soc. Dalton Trans.* **1998**, 2169–2176.

[7] M. L. Creber, K. G. Orrell, A. G. Osborne, V. Sik, M. B. Hursthouse, K. M. A. Malik, *J. Chem. Soc. Dalton Trans.* **2000**, 4218–4226.

[8] P. J. Heard, J. Cameron, *J. Chem. Soc. Dalton Trans.* **1997**, 1083–1091.

[9] P. J. Heard, P. M. King, A. D. Bain, P. Hazendonk, D. A. Tocher, *J. Chem. Soc. Dalton Trans.* **1999**, 4495–4501.

[10] J. H. Groen, P. W. N. M. van Leeun, K. Vrieze, *J. Chem. Soc. Dalton Trans.* **1998**, 113–117.

[11] a) S. J. Chadwell, S. J. Coles, P. G. Edwards, M. B. Hursthouse, *J. Chem. Soc. Dalton Trans.* **1996**, 1105–1112; b) R. Jaouhari, P. G. Edwards, *Recl. Trav. Chim. Pays-Bas* **1988**, *107*, 511–513; c) N. W. Alcock, A. W. G. Platt, P. Pringle, *J. Chem. Soc. Dalton Trans.* **1987**, 2273–2280; d) J. P. Farr, F. E. Wood, A. L. Balch, *Inorg. Chem.* **1983**, *22*, 3387–3393.

[12] a) T. B. Rauchfuss, J. Clements, S. F. Agnew, D. M. Roundhill, *Inorg. Chem.* **1977**, *16*, 775–778; b) E. Lindner, U. Schober, R. Fawzi, W. Hiller, U. Englert, P. Wegner, *Chem. Ber.* **1987**, *120*, 1621–1628; c) L. Horner, G. Simons, *Z. Naturforsch. B: Anorg. Chem. Org. Chem.* **1984**, *39*, 497–503; d) M. Alvarez, N. Lugan, R. Mathieu, *J. Organomet. Chem.* **1994**, *468*, 249–256; e) B. D. Vineyard, W. S. Knoweles, M. J. Sabacky, G. L. Bachman, D. J. Weinkauff, *J. Am. Chem. Soc.* **1977**, *99*, 5946–5952; f) H. Yang, M. Alvarez-Gressier, N. Lugan, R. Mathieu, *Organometallics* **1997**, *16*, 1401–1409; g) H. Yang, M. Alvarez, N. Lugan, R. Mathieu, *J. Chem. Soc. Chem. Commun.* **1995**, 1721–1722; h) M. A. Esteruelas, A. M. Lòpez, L. A. Oro, A. Perez, M. Schulz, H. Werner, *Organometallics* **1993**, *12*, 1823–1830; i) E. Lindner, Q. Wang, H. A. Mayer, A. Bader, H. Kühbauch, P. Wegner, *Organometallics* **1993**, *12*, 3291–3296; j) J. M. Brown, P. A. Chaloner, G. Descotes, R. Glaser, D. Lafont, D. Sinou, *J. Chem. Soc. Chem. Commun.* **1979**, 611–613.

[13] a) E. Lindner, S. Meyer, P. Wegner, B. Karle, A. Sickinger, B. Steger, *J. Organomet. Chem.* **1987**, *335*, 59–70; b) E. Lindner, A. Sickinger, P. Wegner, *J. Organomet. Chem.* **1986**, *312*, C37–C40; c) R. W. Wegman, A. G. Abatjoglou, A. M. Harrison, *J. Chem. Soc. Chem. Commun.* **1987**, 1891–1892; d) E. Lindner, H. A. Mayer, P. Wegner, *Chem. Ber.* **1986**, *119*, 2616–2630; e) S. Bischoff, A. Weigt, H. Miebner, B. Lücke, *J. Mol. Catal.* **1996**, *107*, 339–346; f) J. Freiberg, A. Weigt, H. Dilcher, *J. Prakt. Chem.* **1993**, *335*, 337–344; g) E. Lindner, A. Bader, H. Bräunling, R. Jira, *J. Mol. Catal.* **1990**, *57*, 291–300; h) E. Lindner, A. Bader, E. Glaser, P. Wegner, *J. Mol. Catal.* **1989**, *56*, 86–94; i) E. Lindner, J.-P. Reber, *Z. Naturforsch. B: Anorg. Chem. Org. Chem.* **1991**, *46b*, 1581–1584; j) E. Lindner, H. Norz, *Chem. Ber.* **1990**, *123*, 459–465.

[14] a) M. Alvarez, N. Lugan, B. Donnadieu, R. Mathieu, *Organometallics* **1995**, *14*, 365–370; b) C. Abu-Gnim, I. Amer, *J. Chem. Soc. Chem. Commun.* **1994**, 115–117; c) C. Abu-Gnim I. Amer, *J. Mol. Catal.* **1993**, *85*, L275–L278; d) S. Gladiali, L. Pinna, C. G. Arena, E. Rotondo, F. Faraone, *J. Mol. Catal.* **1991**, *66*, 183–190.

[15] S. Meking, W. Keim, *Organometallics* **1996**, *15*, 2650–2656.

[16] a) H. Adams, N. A. Bailey, M. Colley, P. A. Scofield, C. White, *J. Chem. Soc. Dalton Trans.* **1994**, 1445–1451; b) M. C. Bonnet, B. Stitou, I. Tkatchenko, *J. Organomet. Chem.* **1985**, *279*, C1–C4.

[17] K. Burgess, M. J. Ohlmeyer, K. H. Whitmire, *Organometallics* **1992**, *11*, 3588–3600.

[18] M. Bressan, A. Morvillo, *J. Chem. Soc. Chem. Commun.* **1988**, 650–651.

[19] a) G. P. C. M. Dekker, A. Buijs, C. J. Elsevier, K. Vrieze, P. W. N. M. van Leeuwen, W. J. J. Smeets, A. J. Spek, Y. F. Wang, C. H. Stam, *Organometallics* **1992**, *11*, 1937–1948; b) S. Park, D. Hedden, H. M. Roundhill, *Organometallics* **1986**, *5*, 2151–2152; c) E. Lindner, B. Keppeler, H. A. Mayer, K. Gierling, R. Fawzi, M. Steimann, *J. Organomet. Chem.* **1996**, *526*, 175–186; d) H. Werner, M. Schulz, B. Windmüller, *Organometallics* **1995**, *14*, 3659–3668.

[20] K. R. Dunbar, S. C. Haefner, A. Quillevèrè, *Polyhedron* **1990**, *9*, 1695–1702; K. R. Dunbar, *Comments Inorg. Chem.* **1992**, *13*, 313–357.

[21] R. S. Vagg, in Comprehensive Coordination Chemistry: The *Synthesis* Reactions, Properties & Application of Coordination Compounds, G. Wilkinson, R. G. Gillard, J. A. McCleverty, Eds., Pergamon, Oxford, UK, **1987**, Vol. 2, pp 793–812.

[22] a) E. C. Constable, R. P. G. Henney, D. A. Tocher, *J. Chem. Soc. Chem. Commun.* **1989**, 913–914; b) E. C. Constable, S. J. Dunne, D. G. F. Rees, C. X. Schmitt, *J. Chem. Soc. Chem. Commun.* **1989**, 1169–1170; c) E. C. Constable, R. P. G. Henney, D. A. Tocher, *J. Chem. Soc. Dalton Trans.* **1992**, 2467–2474.

[23] E. W. Abel, D. Ellis, K. G. Orrell, *J. Chem. Soc. Dalton Trans.* **1992**, 2243- 2249.

[24] E. W. Abel, P. J. Heard, K. G. Orrell, M. B. Hursthouse, M. A. Mazid, *J. Chem. Soc. Dalton Trans.* **1993**, 3795–3801.

[25] E. W. Abel, E. S. Blackwall, M. L. Creber, P. J. Heard, K. G. Orrell, *J. Organomet. Chem.* **1995**, *490*, 83–88.

[26] a) D. C. Black, *Aust. J. Chem.* **1967**, *20*, 2101–2107; b) R. Driver, W. R. Walker, *Aust. J. Chem.* **1968**, *21*, 2101–2107; c) M. E. Bridson, W. R. Walker, *Aust. J. Chem.* **1970**, *23*, 1191–1197; d) G. C. Pappalardo, A. Seminara, *J. Inorg. Nucl. Chem.* **1976**, *38*, 1993 – 1995; e) A. Forchioni, V. Librando, G. C. Pappalardo, *J. Chem. Soc. Dalton Trans.* **1977**, 638–641; f) F. Nicolò, G. Bruno, G. Tresoldi, *Acta Crystallogr. Sect C* **1996**, *52*, 2188–2191; g) M. Kondo, S. Kawata, S. Kitagawa, H. Kiso, M. Munukata, *Acta Crystallogr. Sect C* **1995**, *51*, 567–569; h) O. S. Jung, D. H. Jo, Y. A. Lee, B. J. Conklin, C. G. Pierpoint, *Inorg. Chem.* **1997**, *36*, 19–24; i) G. Tresoldi, S. Lo Schiavo, P. Piraino, *Inorg. Chim. Acta* **1997**, *254*, 381–385.

[27] a) G. Bruno, F. Nicolò, G. Tresoldi, *Acta Crystallogr. Sect C* **2000**, *56*, 282- 283; b) G. Bruno, F. Nicolò, G. Tresoldi, S. Lanza, *Acta Crystallogr. Sect C* **2002**, *58*, M56–M58.

[28] G. Bruno, F. Nicolò, S. Lo Schiavo, M. S. Sinicropi, G. Tresoldi, *J. Chem. Soc. Dalton Trans.* **1995**, 17–24.

[29] G. Tresoldi, E. Rotondo, P. Piraino, M. Lanfranchi, A. Tiripicchio, *Inorg. Chim. Acta* **1992**, *194*, 233–241.

[30] G. Tresoldi, P. Piraino, E. Rotondo, F. Faraone, *J. Chem. Soc. Dalton Trans.* **1991**, 425–430.

[31] G. De Munno, G. Bruno, E. Rotondo, G. Giordano, S. Lo Schiavo, P. Piraino, G. Tresoldi, *Inorg. Chim. Acta* **1993**, *208*, 67–75.

[32] G. Tresoldi, S. Lo Schiavo, P. Piraino, P. Zanello, *J. Chem. Soc. Dalton Trans.* **1996**, 885–892.

[33] W. M. Teles, N. G. Fernandes, A. Abras, C. A. L. Filgueiras, *Trans. Met. Chem.* **1999**, *24*, 321–325.

[34] R. J. Anderson P. J. Steel, *Acta Crystallogr. Sect C* **1996**, *54*, 2188- 2191.

[35] R. Scopelliti, G. Bruno, C. Donato, G. Tresoldi, *Inorg. Chim. Acta* **2001**, *313*, 43–55.

[36] G. Tresoldi, S. Lo Schiavo, S. Lanza, P. Cardiano, *Eur. J. Inorg. Chem.* **2002**, 181–191.
[37] L. Baradello, S. Lo Schiavo, F. Nicolò, S. Lanza, G. Alibrandi, G. Tresoldi, *Eur. J. Inorg. Chem.* **2004**, 3358–3369.
[38] E. W. Abel, S. K. Bhargava, K. G. Orrell, *Prog. Inorg. Chem.* **1984**, *32*, 1–118.
[39] G. Binsch, H. Kessler, *Angew. Chem. Int. Ed. Engl.* **1980**, *19*, 411–494.
[40] F. Haviv, R. W. DeNet, R. J. Micaels, J. J. D. Ratajczyk, G. W. Carter, P. R. Young, *J. Med. Chem.* **1983**, *26*, 218–222.

Received: November 23, 2004